

RESEARCH COMMUNICATION

Crystal structure of the phosphatidylinositol 3,4-bisphosphate-binding pleckstrin homology (PH) domain of tandem PH-domain-containing protein 1 (TAPP1): molecular basis of lipid specificityChristine C. THOMAS*, Simon DOWLER†, Maria DEAK†, Dario R. ALESSI† and Daan M. F. VAN AALTEN*¹

*Division of Biological Chemistry and Molecular Microbiology, Wellcome Trust Biocentre, School of Life Sciences, University of Dundee, Dow Street, Dundee DD1 5EH, Scotland, U.K., and †MRC Protein Phosphorylation Unit, Wellcome Trust Biocentre, School of Life Sciences, University of Dundee, Dow Street, Dundee DD1 5EH, Scotland, U.K.

Phosphatidylinositol 3,4,5-trisphosphate [PtdIns(3,4,5) P_3] and its immediate breakdown product PtdIns(3,4) P_2 function as second messengers in growth factor- and insulin-induced signalling pathways. One of the ways that these 3-phosphoinositides are known to regulate downstream signalling events is by attracting proteins that possess specific PtdIns-binding pleckstrin homology (PH) domains to the plasma membrane. Many of these proteins, such as protein kinase B, phosphoinositide-dependent kinase 1 and the dual adaptor for phosphotyrosine and 3-phosphoinositides (DAPP1) interact with both PtdIns(3,4,5) P_3 and PtdIns(3,4) P_2 with similar affinity. Recently, a new PH-domain-containing protein, termed tandem PH-domain-containing protein (TAPP) 1, was described which is the first protein reported to bind PtdIns(3,4) P_2 specifically. Here we describe the crystal structure of the PtdIns(3,4) P_2 -binding PH domain of

TAPP1 at 1.4 Å (1 Å = 0.1 nm) resolution in complex with an ordered citrate molecule. The structure is similar to the known structure of the PH domain of DAPP1 around the D-3 and D-4 inositol-phosphate-binding sites. However, a glycine residue adjacent to the D-5 inositol-phosphate-binding site in DAPP1 is substituted for a larger alanine residue in TAPP1, which also induces a conformational change in the neighbouring residues. We show that mutation of this glycine to alanine in DAPP1 converts DAPP1 into a TAPP1-like PH domain that only interacts with PtdIns(3,4) P_2 , whereas the alanine to glycine mutation in TAPP1 permits the TAPP1 PH domain to interact with PtdIns(3,4,5) P_3 .

Key words: phosphatidylinositide, protein structure, signalling.

INTRODUCTION

The 3-phosphoinositides phosphatidylinositol 3,4,5-trisphosphate [PtdIns(3,4,5) P_3] and PtdIns(3,4) P_2 function as cellular second messengers. Their concentrations are increased following stimulation of cells with extracellular agonists, and they are thought to trigger the activation of signal transduction networks that regulate a plethora of processes, including physiological responses to insulin and control of cell survival [1,2]. PtdIns(3,4,5) P_3 is generated following growth factor/insulin-induced activation of members of the phosphoinositide 3-kinase (PI 3-kinase) family, which phosphorylate PtdIns(4,5) P_2 at the D-3 position of the inositol ring [2]. PtdIns(3,4,5) P_3 can then be converted either back into PtdIns(4,5) P_2 through the action of a 3-phosphatase termed PTEN [3] or through the action of 5-phosphatases termed SH2-containing inositol phosphatase (SHIP) 1 or SHIP2 into PtdIns(3,4) P_2 [4]. Recent work indicates that PtdIns(3,4) P_2 can also be generated via a PI 3-kinase-independent pathway in response to agonists such as hydrogen peroxide [5] and cross-linking of platelet integrin receptors [6]. Much progress has been made on dissecting the molecular mechanisms by which PtdIns(3,4,5) P_3 /PtdIns(3,4) P_2 trigger physiological processes, following the discovery that a specialized module, termed the pleckstrin homology (PH) domain, is used by proteins to interact with these 3-phosphoinositides [7]. Proteins that possess PH

domains that can interact with PtdIns(3,4,5) P_3 include those found on the serine/threonine-specific protein kinases, protein kinase B and the phosphoinositide-dependent kinase 1 [8], the Bruton's tyrosine kinase (BTK) family of tyrosine kinases [9], certain adaptor proteins such as dual adaptor for phosphotyrosine and 3-phosphoinositides (DAPP1) [10–13] and the Grb2-associated binder-1 [14], as well as the ADP-ribosylation factor (ARF), the GTPase-activating protein centaurin- α [15] and the ARF guanine-nucleotide-exchange factor, general receptor for phosphoinositides-1 (GRP1) [16]. These are recruited to the plasma membrane following stimulation of cells with agonists that activate PI 3-kinase, where they are brought into the vicinity of their physiological effectors and/or are activated by phosphorylation at this location (reviewed in [8]). Although there are now estimated to be approx. 250 proteins in the human genome that possess a PH domain (S. Dowler and D. R. Alessi, unpublished work), only a small proportion of these are thought to specifically interact with PtdIns(3,4,5) P_3 and/or PtdIns(3,4) P_2 . All of the PH domains whose structures have been determined so far possess a conserved fold in which the N-terminal 80% of the protein forms two orthogonally arranged β -sheets, one that contains four strands (1–4), and one that contains three strands (5–7), whereas the C-terminal region forms an amphipathic α -helix [7]. The structure of three PtdIns(3,4,5) P_3 -binding PH domains, namely, BTK [17], DAPP1 [18] and GRP1

Abbreviations used: ARF, ADP-ribosylation factor; BTK, Bruton's tyrosine kinase; DAPP1, dual adaptor for phosphotyrosine and 3-phosphoinositides; GST, glutathione S-transferase; PH, pleckstrin homology; PI 3-kinase, phosphoinositide 3-kinase; SHIP, SH2-containing inositol phosphatase; GRP1, general receptor for phosphoinositides-1; TAPP, tandem PH-domain-containing protein; TAPP1-PH_{CT}, PtdIns(3,4) P_2 -binding PH domain of TAPP1; VL, variable loop.

¹ To whom correspondence should be addressed (e-mail dava@davapc1.bioch.dundee.ac.uk).

The coordinates and structure factors will appear in the PDB under the accession numbers 1eaz and r1eazsf respectively.

[18,19], have been solved complexed to the inositol head group of PtdIns(3,4,5) P_3 , inositol(1,3,4,5)-tetrakisphosphate [Ins(1,3,4,5) P_4]. These structures have provided insight into the molecular details of the PtdIns(3,4,5) P_3 -PH domain interaction. The side chains of the $\beta 1$ - $\beta 2$ and $\beta 6$ - $\beta 7$, and in some cases $\beta 3$ - $\beta 4$, connecting loops form the inositol phosphate head group binding site. These loops are the most variable in length and sequence between PH domains and have been termed the variable loops VL1, VL2 and VL3 [20]. The basic amino acids in these loops form direct interactions with specific monoester phosphate groups of the phosphoinositol head group of PtdIns(3,4,5) P_3 [7]. The structures elegantly explain why the PH domains of BTK [17] and GRP1 [18,19] can only interact with PtdIns(3,4,5) P_3 , and not PtdIns(3,4) P_2 , as the high affinity binding is mediated through interactions of the 5-phosphate on PtdIns(3,4,5) P_3 with basic residues on BTK and GRP1 PH domains. In contrast, the DAPP1 PH domain interacts with similar affinity to both PtdIns(3,4,5) P_3 and PtdIns(3,4) P_2 . It can do so because the DAPP1 PH domain, unlike those of GRP1 and BTK, forms high affinity interactions with the 3- and 4-phosphate groups of the inositol ring and not with the 5-phosphate group that is accommodated in a largely empty space in the ligand-binding pocket [18].

We recently described two related novel proteins termed **tandem PH-domain-containing protein (TAPP) 1** and **TAPP2**, because they possessed two sequential PH domains [21]. The N-terminal PH domains of TAPP1 and TAPP2 did not interact with any phosphoinositide tested, whereas the C-terminal PH domain bound PtdIns(3,4) P_2 with high affinity, but did not bind significantly to PtdIns(3,4,5) P_3 or any other phosphoinositide tested in a quantitative surface plasmon resonance based assay [21]. It cannot be ruled out, however, that TAPP1 and/or TAPP2 may also possess weak affinity for PtdIns(3,4,5) P_3 as Ferguson et al. [18] have shown that the inositol head group of PtdIns(3,4,5) P_3 , Ins(1,3,4,5) P_4 , can interact with the C-terminal PH domain of TAPP1 albeit with much weaker apparent affinity than Ins(1,3,4) P_3 , the head group of PtdIns(3,4) P_2 . In a qualitative protein-lipid overlay, TAPP1 can also be shown to interact weakly with high concentrations of PtdIns(3,4,5) P_3 ([21] and the present study). The physiological functions of TAPP1 and TAPP2 are unknown, but these proteins may mediate cellular responses that are triggered by PtdIns(3,4) P_2 . Here, we investigate the structural basis of the unusual specificity of the C-terminal PH domain of TAPP1, and describe the crystal structure of this domain at 1.4 Å (1 Å = 0.1 nm) resolution, together with a detailed structure-based mutagenesis study, which reveal key residues that enable TAPP1 to bind PtdIns(3,4) P_2 specifically. The structure was solved in complex with an ordered citrate molecule, which could potentially provide a scaffold for PtdIns mimetics with possible chemotherapeutic potential.

MATERIALS AND METHODS

Materials

All of the phosphoinositides used in this study were dipalmitoyl derivatives obtained from Echelon (Salt Lake City, UT, U.S.A.). Hybond-C extra, the pGEX4T-1 vector, enhanced chemiluminescence reagent, thrombin protease and glutathione-Sepharose were from Amersham Pharmacia Biotech. Protease inhibitor tablets were from Roche. Benzamidine-agarose and monoclonal anti-[glutathione S-transferase (GST)] were antibody from Sigma. Horseradish peroxidase-conjugated goat anti-mouse secondary antibody was from Pierce. VivaSpin concentrators were from Vivascience (Lincoln, U.K.).

General methods and Buffers

Restriction enzyme digests, DNA ligations, PCR cloning and site-directed mutagenesis were performed using standard protocols. All DNA constructs were verified by DNA sequencing (The Sequencing Service, School of Life Sciences, University of Dundee, Dundee, Scotland, U.K.). Buffer A contains 50 mM Tris/HCl, pH 7.5, 1 mM EGTA, 1 mM EDTA, 1 mM sodium orthovanadate, 10 mM sodium- β -glycerophosphate, 50 mM NaF, 5 mM dithiothreitol and 'complete' proteinase inhibitor cocktail (one tablet per 25 ml; Roche). Buffer B contains 50 mM Tris/HCl, pH 7.5, 0.1 mM EGTA, 0.2 M NaCl and 5 mM dithiothreitol. Buffer C contains 50 mM Mes/NaOH, pH 6.0, 150 mM NaCl and 0.1% (w/v) Tween-20.

Preparation of PH domain expression constructs

The PtdIns(3,4) P_2 -binding PH domain of TAPP1 (TAPP1-PH_{CT}) was amplified by PCR using the Hi-fidelity PCR system with the full-length TAPP1 cDNA [21] as the template, and the 5'-primer GATCCATGTTTACTCCTAAACCACCTCAAGATAG and the 3'-primer GGATCCTCAGGGATGCTCAGAAGACGCA GATCT. This amplified a length of DNA encoding residues 182-304 of human TAPP1 with a stop codon immediately after position 304 which is equivalent in length to the DAPP1 PH domain fragment that was crystallized previously [18]. This fragment was subcloned into the *Bam*H1 restriction site of the *Escherichia coli* expression vector pGEX4T-1. The resultant construct encodes for the bacterial expression of TAPP1-PH_{CT} with an N-terminal GST tag. This construct was used for both crystallization and for generating the mutants of TAPP1-PH_{CT} employed in the lipid-binding experiments shown in Figure 3. The pGEX4T-1 construct encoding for the expression of the GST-fusion protein of the isolated PH domain of human DAPP1 (residues 154-273) was as described previously [10], and was used to generate the pGEX4T-1 construct expressing the isolated GST-DAPP1[Gly¹⁷⁶ → Ala] mutant PH domain.

Expression and purification of TAPP1-PH_{CT} for crystallization

E. coli BL21 cells transformed with the pGEX4T-1 vector encoding the expression of GST-TAPP1-PH_{CT} were grown at 37 °C in 2 litres of Luria-Bertani broth with 50 μ g/ml carbenicillin until D_{600} reached 0.7. The expression of GST-TAPP1-PH_{CT} was induced by the addition of 250 μ M isopropyl β -D-thiogalactopyranoside, and the bacteria were then grown for a further 18 h at 27 °C. The cells were harvested by centrifugation at 3500 g for 15 min, then lysed by resuspension in 100 ml of Buffer A containing DNase and lysozyme and passing through a French Press. The resulting solution was centrifuged at 13000 g for 30 min to remove residual debris, briefly sonicated and passed through a 0.45 μ m-pore-size filter. The supernatant was incubated for 1 h at 4 °C in 4 ml of glutathione-Sepharose equilibrated previously in Buffer A. The beads were then washed 4 times with 5 column volumes of Buffer A, and subsequently washed 6 times with 5 column volumes Buffer B. The TAPP1-PH_{CT} domain was then separated from the GST-tag by incubating the glutathione-Sepharose beads conjugated to GST-TAPP1-PH_{CT} in a 1:1 volume ratio of resin/Buffer B with 100 units/ml thrombin at 4 °C overnight. The resin was centrifuged, washed twice with 2 volumes of Buffer B and the combined supernatants containing TAPP1-PH_{CT} were applied to a 0.2 ml benzamidine-agarose column to remove the thrombin. The eluate from this column was subsequently applied to a 1 ml glutathione-Sepharose column equilibrated in Buffer B to remove trace contamination of GST. The yield obtained was approximately

Table 1 Details of data collection and refinement

All measured data were included in the refinement. R.M.S., root mean square.

Parameter	Value
Space group	C222 ₁
Unit cell (Å)	<i>a</i> = 65.02 <i>b</i> = 102.80 <i>c</i> = 41.47
Resolution, last bin (Å)	30–1.4 (1.45–1.4)
Unique reflections	27661
Redundancy	4.0 (3.1)
Completeness (%)	98.9 (97.7)
<i>R</i> _{merge}	0.058 (0.115)
<i>I</i> / <i>σ</i> <i>I</i>	21.7 (4.2)
<i>R</i> _{cryst}	0.171
<i>R</i> _{free}	0.228
Number of atoms	
protein	874
water	134
Wilson B-factor (Å ²)	20.1
protein (Å ²)	26.9
(water)	44.1
R.M.S. deviations from ideal geometry	
Bond lengths (Å)	0.010
Bond angles (°)	1.98
Main chain B-factors (Å ²)	2.93

8 mg of TAPP1-PH_{CT} domain per 2 litres of *E. coli* culture. TAPP1-PH_{CT} was analysed by SDS/PAGE followed by Coomassie Brilliant Blue staining of the gel, and was found to be essentially homogeneous. It was analysed by electrospray mass spectroscopy, revealing a major single species with a molecular mass of 14138.39 Da, close to the predicted mass of 14162.24 Da for the TAPP1-PH_{CT} fragment.

Crystallization and data collection

The TAPP1-PH_{CT} protein was concentrated to a final concentration of 14.5 mg/ml (as determined by a Bradford assay) using a VivaSpin concentrator. Hanging drops were formed by mixing 1 μl of protein solution with 1 μl of a mother liquor solution containing 0.085 M sodium citrate, pH 5.6, 25.5% (w/v) PEG 4000, 15% (v/v) glycerol and 0.17 M ammonium acetate. The drop was then equilibrated by vapour diffusion against a reservoir containing mother liquor. Crystals were grown at 20 °C and appeared after 1 day, growing to 0.3 mm × 0.15 mm × 0.1 mm over 6 days. Crystals were frozen straight from the drop without additional cryo protection. Data were collected to 1.4 Å at the European Synchrotron Radiation Facility (Grenoble, France) beamline ID14-EH4, using an ADSC Q4 CCD detector, at a wavelength of 1.0 Å. The temperature of the crystals was maintained at 100 K using a nitrogen cryostream. Data were processed using the HKL package [22], statistics are shown in Table 1.

Structure determination and refinement

The structure of the TAPP1 PH domain was solved by molecular replacement with AMoRe [23], using the DAPP1 structure [18] as a search model. A single solution was obtained with an *R*-factor of 0.501 and a correlation coefficient of 0.392. The resulting model phases were used as the input for warpNtrace [24] which was able to build 92 out of the 123 possible residues. Iterative model building in O [25] together with refinement in CNS

reduced the *R*-factor to 0.213 (*R*_{free} = 0.231). Refinement was then continued with SHELX97 [26], incorporating anisotropic B-factors, and as a last step riding hydrogens, resulting in the final model with an *R*-factor of 0.171 (*R*_{free} = 0.228) (Table 1).

Protein–lipid overlay assay

The wild-type and mutant PH domains of TAPP1 and DAPP1 used for the lipid-binding experiments were expressed in *E. coli* and purified as described previously [21]. Lipid-binding studies were carried out using the protein–lipid overlay assay described previously [10,21]. Briefly, freeze-dried lipids were reconstituted in a 1:1 (v/v) mixture of chloroform/methanol at a concentration of 1 mM. The stock solution was serially diluted by 2-fold in a mixture of chloroform/methanol/water (1:2:0.8, by vol.) and 1 μl of this solution, corresponding to between 1 pmol to 1 nmol of phosphoinositide, was spotted on to HybondC-extra nitrocellulose membrane, which was allowed to dry at room temperature for 1 h. Membranes were blocked for 1 h at room temperature in Buffer C containing 2% (w/v) BSA, and were then incubated in Buffer C containing 2% BSA and 10 nM of the indicated purified wild-type or mutant GST-fusion PH domains of DAPP1 and TAPP1. After overnight incubation at 4 °C with gentle rocking, the membranes were washed 5 times during a 40 min period in Buffer C, then incubated with a 1:2000 dilution of a monoclonal anti-GST antibody in Buffer C containing 2% BSA for 1 h at room temperature. Membranes were washed a further 5 times during a 40 min period in Buffer C and then incubated with a 1:5000 dilution of horseradish peroxidase-conjugated goat anti-mouse secondary antibody in Buffer C containing 2% BSA for 1 h. The membranes were washed 8 times over 1 h and detection of GST-fusion proteins bound to the membrane was achieved using enhanced chemiluminescence.

RESULTS AND DISCUSSION

Overall structure of the TAPP1 PH domain

The C-terminal PtdIns(3,4)P₂-binding PH domain of human TAPP1 (residues 182–304, termed TAPP1-PH_{CT}) was expressed in *E. coli*, purified and crystallized as described in the Materials and methods section. Its structure was solved by molecular replacement and refined to 1.4 Å resolution with *R*_{cryst} = 0.171 and *R*_{free} = 0.228 (Figure 1A and Table 1). As expected, the overall fold of the protein is similar to that determined previously for PH domain structures [7]. Strands β1–β4 are arranged in an anti-parallel fashion, forming a sheet, which is approximately stacked orthogonally on to another sheet formed by strands β5–β7 and β1. One open end of this β-clamp structure is covered by the C-terminal helix. Like other PH domain structures, the other open end is surrounded by loops β1–β2, β3–β4 and β6–β7, also termed VL1, VL2 and VL3 respectively. These loops form a bowl shape into which several conserved basic amino acids are clustered, forming the putative phosphoinositide binding site (Figure 1A). Mutation of one of these residues, Arg²¹² to leucine, is known to prevent TAPP1 from binding to PtdIns(3,4)P₂ [21] (Figure 1A). Analysis of surface potential with the program GRASP [27] shows this bowl shape and its associated overall positive charge, whereas on the opposite side of the molecule a cluster of negatively charged residues can be observed (Figure 1B). The resulting dipole is thought to help the orientation and docking of the PH domain on to the negatively charged membrane surface [7].

At the initial stages of the refinement, it became clear that the presumed PtdIns(3,4)P₂ binding pocket was occupied by an ordered small molecule (Figure 1A). This density was not

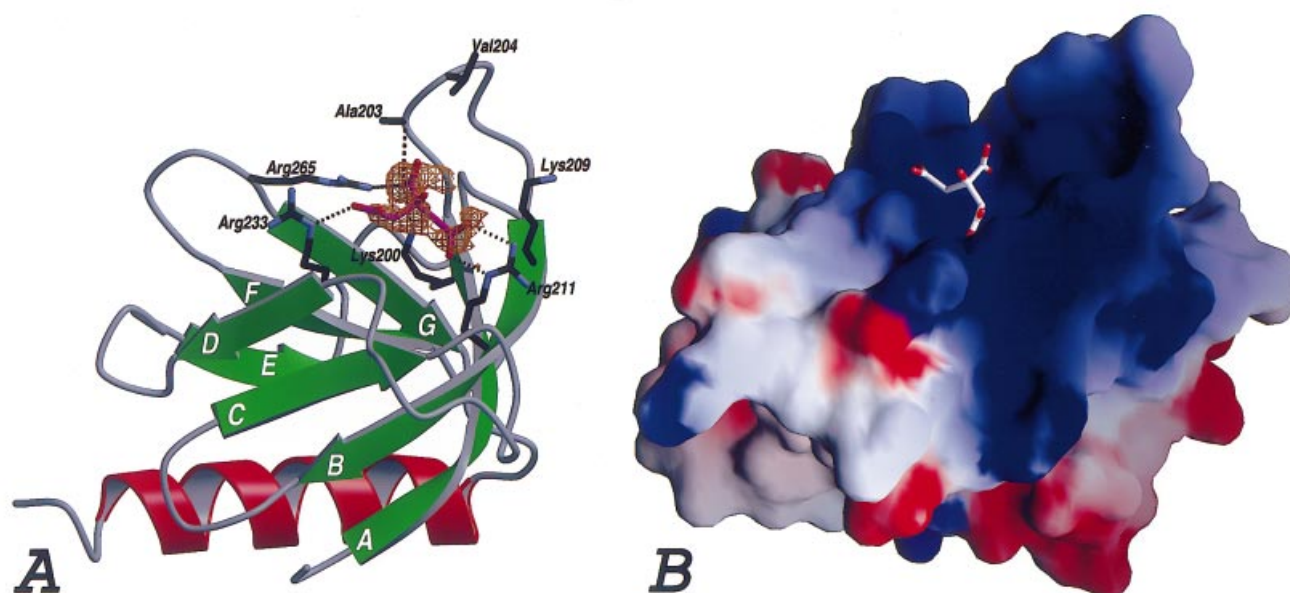


Figure 1 TAPP1 structure

(A) Ribbon drawing of TAPP1-PH_{CT}, with the seven β -strands shown as arrows with letters A–G indicating the order of the strands in the sequence. The C-terminal amphipathic α -helix is shown in red. Side chains of residues in the lipid-head-group-binding pocket are shown in stick representation with black carbons, and the ordered citrate molecule is shown in orange. Hydrogen bonds between citrate and the protein are indicated by black broken lines. The unbiased $F_o - F_c$ difference map (i.e. prior to including a model for the citrate) is shown in orange, contoured at 2.5σ . (B) Electrostatic surface potential calculated with GRASP [27]. Blue areas, +6 kT; red areas, -6 kT. The citrate molecule is shown as a stick model.

interpreted until the last stages of the refinement, when it was modelled as a citrate molecule, which was present at a concentration of 85 mM in the crystallization mother liquor. The carboxylate moieties make several salt bridges with arginines/lysines in the pocket (Figure 1A). Exhaustive soaking experiments of TAPP1-PH_{CT} crystals with Ins(1,3,4) P_3 (the head group of PtdIns(3,4) P_2) were performed. Unfortunately, inspection of $F_o - F_c$ difference maps revealed that the citrate molecule had not been replaced with the soaked head group. In addition numerous, co-crystallization screens with Ins(1,3,4) P_3 did not yield any crystals. The TAPP1-PH_{CT}-citrate complex may provide a scaffold for the design of PtdIns(3,4) P_2 /PtdIns(3,4,5) P_3 mimetics. These compounds could selectively block the recruitment of proteins carrying PH domains to membranes, thus interfering with the signal transduction cascades. Alternatively, they might mimic the effects that phosphoinositides have on these PH domains, thus activating signal transduction cascades. It should be noted that in the crystal structure of DAPP1 and GRP1 PH domains, phosphate and sulphate molecules that were present at high concentrations in the crystallization mother liquor, have also been observed in the 3-phosphoinositide binding site [18,19]. Interestingly, an ordered citrate molecule has also been observed in the structure of a FYVE domain, where it occupies the PtdIns 3-phosphate binding site, although further investigation is required to establish whether this marks the genuine PtdIns 3-phosphate binding site [28].

Comparison of TAPP1-PH_{CT} with the DAPP1 PH domain

A search for structural homologues with DALI [29] confirmed the PH domain of DAPP1 as the most similar structure available

in the PDB, with a root mean square deviation (RMSD) of 1.09 Å on 105 C α atoms. A structure-based sequence alignment of the 3-phosphoinositide-binding PH domains of DAPP1 and TAPP1 is shown in Figure 2(a). The sequence identity between the two PH domains is 37%. VL1, VL2 and VL3 all have the same length in TAPP1 and DAPP1, and exhibit a high degree of sequence conservation. The only significant sequence differences between TAPP1 and DAPP1 in these regions are located in VL1 where a Gly-Leu-Val sequence in DAPP1 is replaced by Ala-Val-Met in TAPP1 (Figure 2a). In order to address whether this difference in sequence between the DAPP1 and TAPP1 PH domains accounts for the ability of DAPP1 to bind both PtdIns(3,4,5) P_3 and PtdIns(3,4) P_2 , whereas TAPP1 can only bind PtdIns(3,4) P_2 , we superimposed the structure of the complex of DAPP1 and inositol (1,3,4,5) P_4 with the equivalent region of TAPP1 (Figure 2b) to generate a model of a TAPP1-PH_{CT}-PtdIns complex (Figure 2b). The 1-, 3- and 4-phosphate groups are surrounded by identical residues (mostly arginines and lysines) in DAPP1 and TAPP1 (Figures 2a and 2b). This includes Arg²¹², whose mutation to a leucine is known to prevent TAPP1 from binding to PtdIns(3,4) P_2 [21] (Figure 2b). In contrast, the positioning of the residues surrounding the 5-phosphate in the PH domain of DAPP1 and TAPP1-PH_{CT} differ significantly. DAPP1 can bind to both PtdIns(3,4,5) P_3 and PtdIns(3,4) P_2 because the 5-phosphate can be accommodated in the ligand-binding pocket. Furthermore, in comparison with the 1-, 3- and 4-phosphate groups (see the Introduction section), the 5-phosphate in the DAPP1-PH-PtdIns(3,4,5) P_3 complex has relatively weak interactions with the protein, through two hydrogen bonds with the backbone nitrogens of Leu¹⁷⁷ and Val¹⁷⁸ (Figure 2b). In the TAPP1-PH_{CT} structure, there is no room for the 5-phosphate to bind. If a 5-phosphate is positioned in TAPP1-PH_{CT} in the same

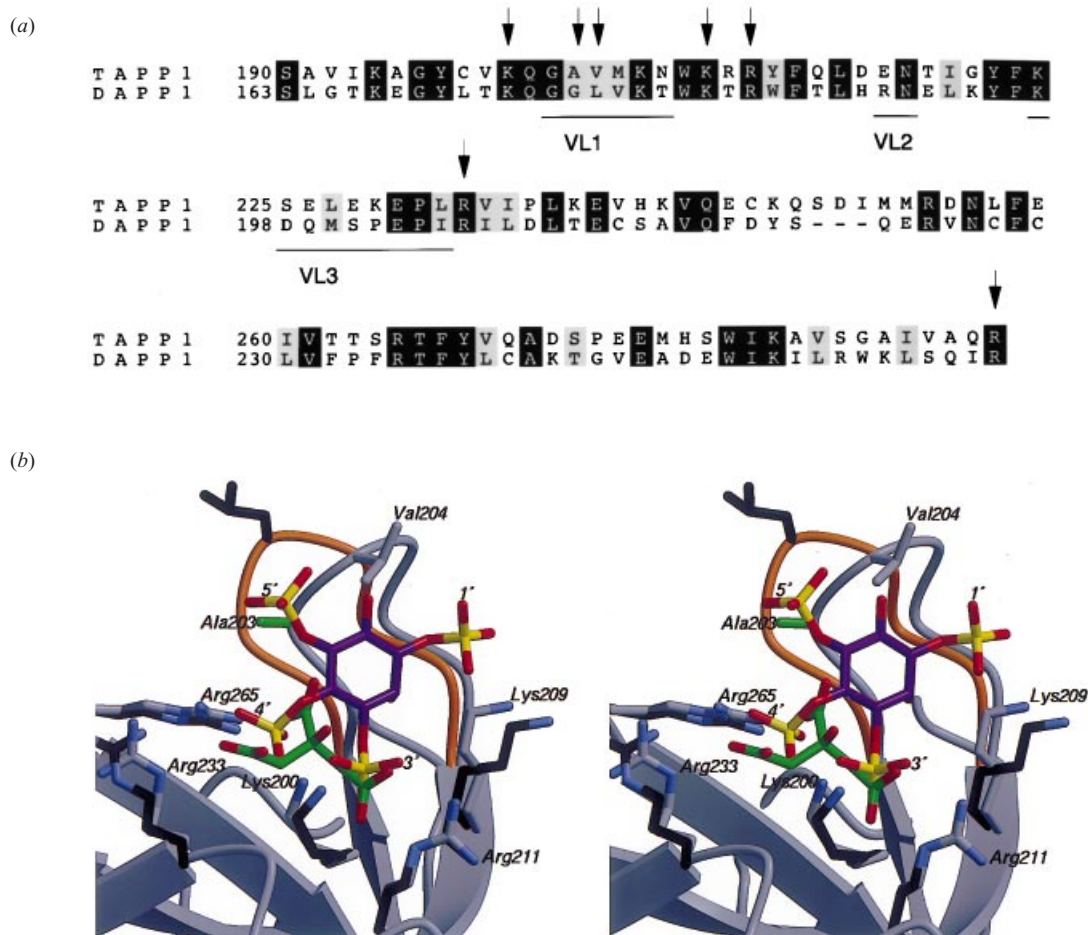


Figure 2 Comparison of the DAPP1 and TAPP1 PH domains

(a) Structure-based sequence alignment of TAPP1 residues 190–253 and DAPP1 residues 163–323. Conserved residues are highlighted in black. Homologous residues are highlighted in grey. Arrows indicate residues in DAPP1 that contact the inositol-lipid head group. Underlined regions indicate the variable loops between the β -strands. (b) Stereo image of the TAPP1/DAPP1 ligand-binding pockets. TAPP1-PH_{CT} is shown as a grey ribbon, with residues lining the ligand-binding pocket drawn in a stick representation with grey carbons. The PtdIns(3,4,5) P_3 head group observed in the DAPP1 structure is shown with the ring in purple and the phosphate groups in yellow and red. DAPP1 VL1 is shown in orange, with residues contacting the inositol head group in black. The ordered citrate molecule observed in the TAPP1-PH_{CT} structure is shown as a stick model with carbons coloured green. Residue Ala²⁰³ in TAPP1, which is mutated to a glycine in DAPP1, is shown in green.

place that it occupies in the DAPP1-PH-Ins(1,3,4,5) P_4 complex, severe clashes are introduced with Ala²⁰³ (equivalent to Gly¹⁷⁶ in DAPP1), with a distance of 1.4 Å between Ala²⁰³-C β and an oxygen on the 5-phosphate (Figure 2b). Another notable steric clash is Val²⁰⁴-C α with an oxygen on the 5-phosphate (2.2 Å). In addition, the two phosphate-backbone hydrogen bonds seen in the DAPP1-PH-Ins(1,3,4,5) P_4 complex can no longer be formed if Ins(1,3,4,5) P_4 is modelled into the TAPP1 phosphoinositide binding site.

It is possible that it is not only the steric effects caused by introduction of a C β atom at position 203 which could prevent TAPP1 interacting with a phosphoinositide bearing a 5-phosphate group. Inspection of the backbone conformation reveals that Gly¹⁷⁶ in DAPP1 lies at $\phi = -83^\circ$, $\psi = -83^\circ$ in the Ramachandran plot, whereas for the equivalent Ala²⁰³ in TAPP1 $\phi = -79^\circ$, $\psi = -31^\circ$. According to the PROCHECK definition [30], the backbone conformation at residue 176 in DAPP1 is near the edge of an 'additional allowed' region in the Ramachandran plot, whereas residue 203 in TAPP1 is near the centre of a highly populated allowed region (right-handed α -helical). Thus it is possible that by the introduction of a C β beyond the glycine

backbone, the VL1 loop is forced into a different conformation to relieve the strain introduced in the backbone. This would cause the observed shifts of up to 4.1 Å in C α positions towards the site of PtdIns binding, resulting in the additional unfavourable changes in interaction with a phosphoinositide bearing a 5-phosphate.

Mutagenesis of residues located in the VL1 loop of the TAPP1 and DAPP1 PH domains

The structural data indicate that mutation of Gly¹⁷⁶ in DAPP1 to alanine, the residue found at the equivalent position in TAPP1, may inhibit the binding of DAPP1 to PtdIns(3,4,5) P_3 , but not affect its interaction with PtdIns(3,4) P_2 . To investigate this possibility, we employed the protein-lipid overlay assay [31,21] in which serial dilutions of phosphoinositides were spotted on to a nitrocellulose membrane and incubated with the isolated PH domain of wild-type DAPP1 and the DAPP1[G176A] mutant. The membranes were then washed and immunoblotted with an anti-GST antibody to detect GST-fusion proteins bound to the membrane by virtue of their interaction with lipid. We dem-

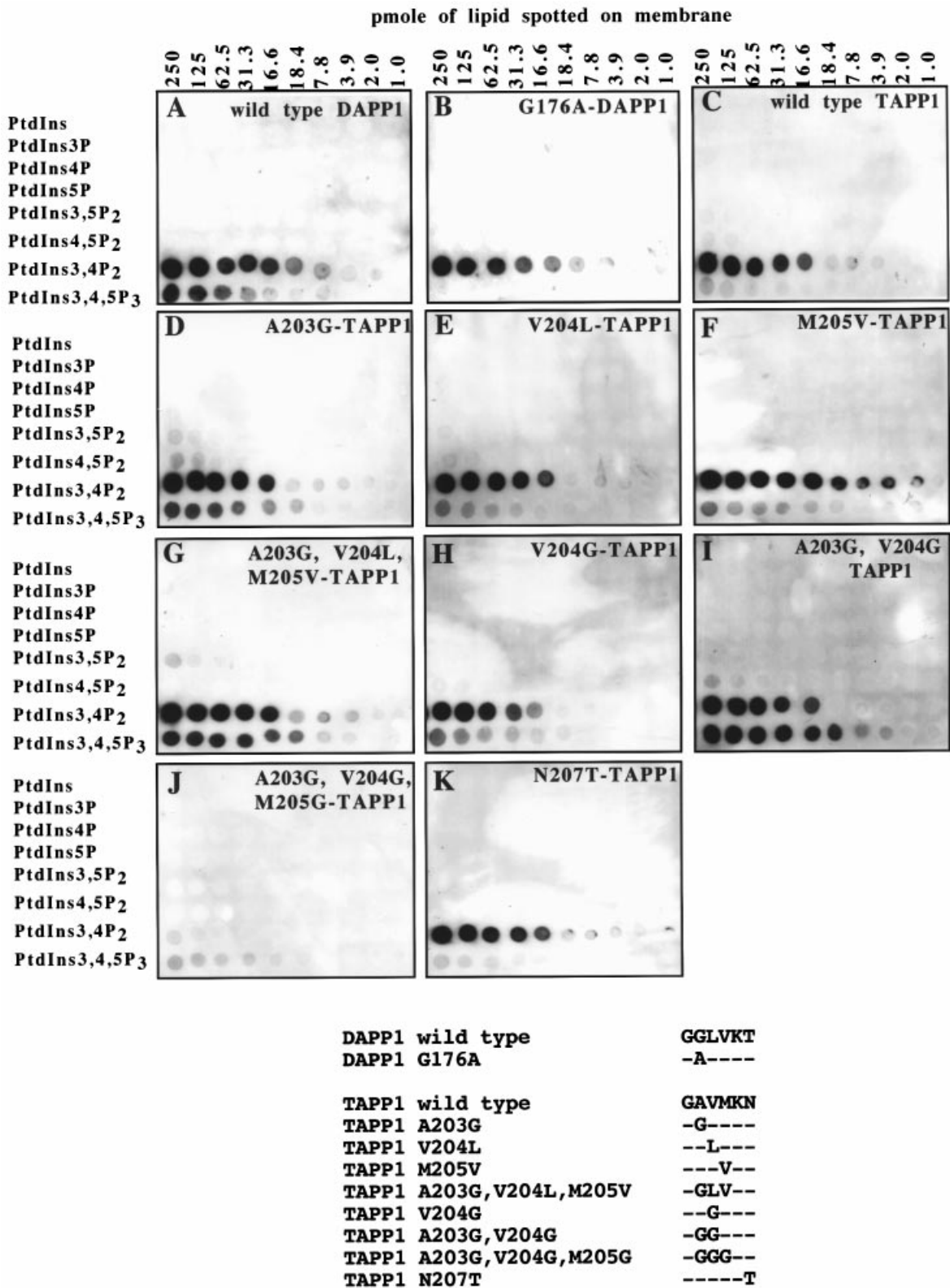


Figure 3 Phosphoinositide-binding properties of wild-type and VL1-mutant DAPP1/TAPP1 PH domains

(A–K) The ability of the indicated GST-fusion proteins to bind a variety of phosphoinositides was analysed using a protein–lipid overlay assay. Serial dilutions of the indicated phosphoinositides were spotted on to nitrocellulose membranes, which were then incubated with the indicated wild-type and mutant purified GST-fusions of the isolated PH domains of the DAPP1 and TAPP1 proteins. The membranes were washed and the GST-fusion proteins bound to the membrane by virtue of their interaction with lipid were detected using an anti-GST antibody. A representative of at least three separate experiments is shown. An alignment of the sequences that encompass the VL1 in TAPP1 and DAPP1 is shown and the mutated residues are indicated. –, Identical residue to the wild-type sequence.

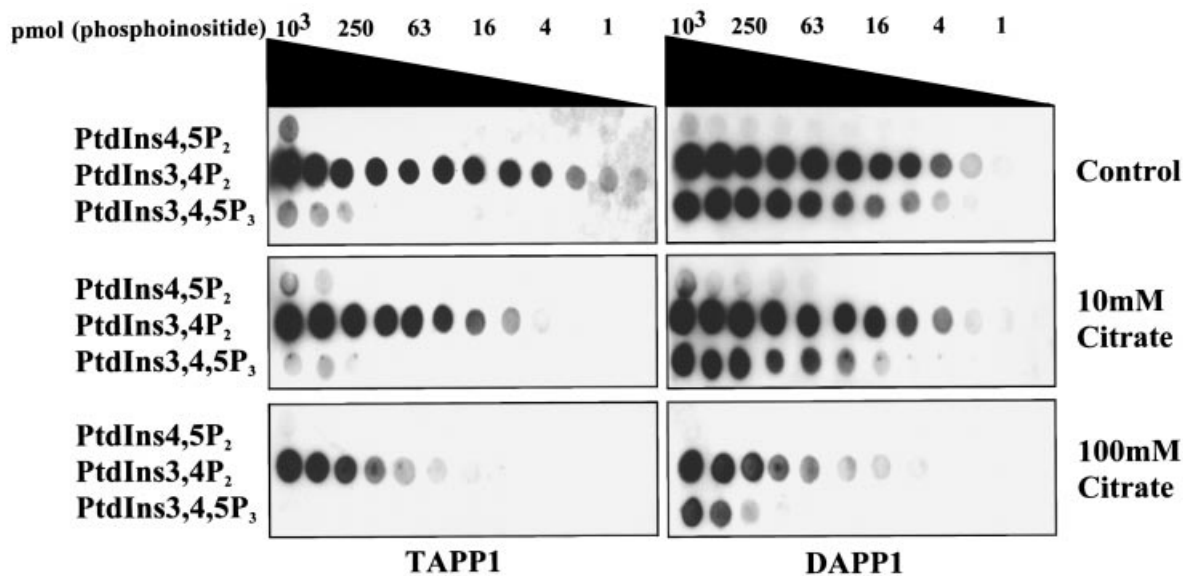


Figure 4 Inhibition of TAPP1 and DAPP1 binding to 3-phosphoinositides by citrate

The ability of GST–TAPP1–PH_{CT} and the GST–DAPP1–isolated PH domains to bind PtdIns(3,4,5) P_3 or PtdIns(3,4) P_2 [or PtdIns(4,5) P_2 as a negative control] in the presence or absence of 10 mM or 100 mM trisodium citrate was analysed using the protein–lipid overlay assay as described in Figure 3, except that the PH domains (10 nM) were incubated for 15 min on ice in the presence of Buffer C containing 2% BSA and 0 mM, 10 mM or 100 mM trisodium citrate. Additional NaCl was added to the samples containing 0 mM and 10 mM trisodium citrate in order to ensure that the ionic strength was the same as the sample containing 100 mM trisodium citrate. Serial dilutions of the indicated phosphoinositides (1 nmol, 500 pmol, 250 pmol, 125 pmol, 63 pmol, 31 pmol, 16 pmol, 8 pmol, 4 pmol, 2 pmol, 1 pmol and 0.5 pmol) were used. Similar results were obtained in three separate experiments.

onstrate that, as reported previously [10,11], wild-type DAPP1 interacts with both PtdIns(3,4,5) P_3 and PtdIns(3,4) P_2 (Figure 3A), but as predicted the mutant DAPP1[G176A] binds to PtdIns(3,4) P_2 (with similar apparent affinity as wild-type DAPP1), but does not bind detectably to PtdIns(3,4,5) P_3 (Figure 3B). A similar situation has been observed in the structure of protein tyrosine phosphatase 1B, which, unlike other tyrosine phosphatases, binds peptides with a tandem of phosphotyrosines [32]. Binding of the second phosphotyrosine is facilitated by introduction of a glycine which creates an extra pocket, harbouring the phosphate group. Mutation of this glycine to large residues significantly impairs binding of peptides with the phosphotyrosine tandem [32].

We next mutated either individually or in combination the residues Ala–Val–Met in the VL1 of TAPP1 to residues present in the equivalent region of DAPP1 (Gly–Leu–Val) to determine whether we could generate a TAPP1 mutant that could interact with PtdIns(3,4,5) P_3 , as well as PtdIns(3,4) P_2 . The TAPP1 mutant in which Ala²⁰³ (the residue equivalent to Gly¹⁷⁶ in DAPP1) was changed to a glycine residue, TAPP1[A203G], showed significant interaction with PtdIns(3,4,5) P_3 compared with the wild-type TAPP1, but still bound to PtdIns(3,4) P_2 with a higher affinity (Figures 3C and 3D). In contrast, the TAPP1[V204L] mutant only interacted with PtdIns(3,4) P_2 (Figure 3E). The TAPP1[M205V] mutant also bound exclusively to PtdIns(3,4) P_2 , with a somewhat higher affinity than wild-type TAPP1 (Figure 3F). A mutant of TAPP1 in which the three residues in the VL1 of TAPP1 (i.e. Ala–Val–Met) were altered to those found in DAPP1 (i.e. Gly–Leu–Val) interacted with moderately higher affinity with PtdIns(3,4,5) P_3 than the TAPP1[A203G] mutant (compare Figures 3D and 3G). We then mutated either individually or in combination further residues in the Ala–Val–Met motif of TAPP1 to glycine residues. The TAPP1[V204G] mutant only interacted with PtdIns(3,4) P_2 like wild-type TAPP1 (Figure

3H). In contrast, the TAPP1[A203G/V204G] mutant interacted with PtdIns(3,4,5) P_3 with significantly higher affinity than the TAPP1[A203G] mutant and, remarkably, even possessed higher affinity for PtdIns(3,4,5) P_3 than PtdIns(3,4) P_2 (Figure 3I). We also generated a mutant TAPP1 in which all three residues in the Ala–Val–Met motif were changed to glycine, but this mutant failed to interact with either PtdIns(3,4) P_2 or PtdIns(3,4,5) P_3 (Figure 3J). To the C-terminus of the Ala–Val–Met sequence in TAPP1 there is a threonine residue (Thr²⁰⁷), whereas in DAPP1 this residue is an asparagine (Asn¹⁸⁰) (Figure 2a). However, this difference does not appear to contribute to the differences in lipid-binding specificity of TAPP1 and DAPP1, because a mutant TAPP1 in which this threonine residue is changed to asparagine still interacted specifically with PtdIns(3,4) P_2 (Figure 3K).

As the TAPP1–PH_{CT} structure obtained had an ordered citrate molecule bound in the lipid-binding pocket (Figures 1A and 2b) and we were unable to obtain crystals of TAPP1 bound to Ins(1,3,4) P_3 , we verified whether citrate could inhibit the binding of TAPP1–PH_{CT} and the isolated PH domain of DAPP1 to 3-phosphoinositides. We observed moderate inhibition at 10 mM citrate, but at a concentration of 100 mM citrate (similar to that present in the crystallization mother liquor) the ability of TAPP1–PH_{CT} to interact with PtdIns(3,4) P_2 and the DAPP1 PH domain to bind PtdIns(3,4,5) P_3 and PtdIns(3,4) P_2 was significantly reduced (Figure 4). As the apparent K_d values of TAPP1 for PtdIns(3,4) P_2 and of DAPP1 for PtdIns(3,4,5) P_3 /PtdIns(3,4) P_2 are estimated to be sub-micromolar [10,21], citrate must therefore interact with these PH domains with $> 10^5$ lower affinity than the natural phosphoinositide ligand(s) of these PH domains. A model of citrate bound to the PH domains of DAPP1 and TAPP1 is shown in Figure 2(b). Together with the structure, these results suggest that polycarboxylates could be used as a scaffold for the design of PH-domain-specific PtdIns mimetics, which could act as activators or inhibitors.

We thank the European Synchrotron Radiation Facility, Grenoble, France, for the allocation of time on beamline ID14-EH4, and the Sequencing Service, School of Life Sciences, University of Dundee for DNA sequencing. D.M.F.v.A. is supported by a Wellcome Trust Career Development Research Fellowship, C.C.T. by a Biotechnology and Biological Sciences Research Council CASE studentship, S.D. by a Medical Research Council (U.K.) Studentship and D.R.A. by the Medical Research Council (U.K.), Diabetes UK and the pharmaceutical companies supporting the Division of Signal Transduction Therapy Unit at the University of Dundee (AstraZeneca, Boehringer Ingelheim, Novo-Nordisk, Pfizer and GlaxoSmithKline).

REFERENCES

- Cantrell, D. A. (2001) Phosphoinositide 3-kinase signalling pathways. *J. Cell Sci.* **114**, 1439–1445
- Leevers, S. J., Vanhaesebroeck, B. and Waterfield, M. D. (1999) Signalling through phosphoinositide 3-kinases: the lipids take centre stage. *Curr. Opin. Cell Biol.* **11**, 219–225
- Simpson, L. and Parsons, R. (2001) PTEN: life as a tumor suppressor. *Exp. Cell Res.* **264**, 29–41
- Erneux, C., Govaerts, C., Communi, D. and Pesesse, X. (1998) The diversity and possible functions of the inositol polyphosphate 5-phosphatases. *Biochim. Biophys. Acta* **1436**, 185–199
- van der Kaay, J., Beck, M., Gray, A. and Downes, C. P. (1999) Distinct phosphatidylinositol 3-kinase lipid products accumulate upon oxidative and osmotic stress and lead to different cellular responses. *J. Biol. Chem.* **274**, 35963–35968
- Banfic, H., Tang, X., Batty, I. H., Downes, C. P., Chen, C. and Rittenhouse, S. E. (1998) A novel integrin-activated pathway forms PKB/Akt-stimulatory phosphatidylinositol 3,4-bisphosphate via phosphatidylinositol 3-phosphate in platelets. *J. Biol. Chem.* **273**, 13–16
- Lemmon, M. A. and Ferguson, K. M. (2000) Signal-dependent membrane targeting by pleckstrin homology (PH) domains. *Biochem. J.* **350**, 1–18
- Vanhaesebroeck, B. and Alessi, D. R. (2000) The PI3K-PDK1 connection: more than just a road to PKB. *Biochem. J.* **346**, 561–576
- Qiu, Y. and Kung, H. J. (2000) Signaling network of the BTK family kinases. *Oncogene* **19**, 5651–5661
- Dowler, S., Currie, R. A., Downes, C. P. and Alessi, D. R. (1999) DAPP1: a dual adaptor for phosphotyrosine and 3-phosphoinositides. *Biochem. J.* **342**, 7–12
- Rao, V. R., Corradetti, M. N., Chen, J., Peng, J., Yuan, J., Prestwich, G. D. and Brugge, J. (1999) Expression cloning of protein targets for 3-phosphorylated phosphoinositides. *J. Biol. Chem.* **274**, 37893–37900
- Marshall, A. J., Niir, H., Lerner, C. G., Yun, T. J., Thomas, S., Disteche, C. M. and Clark, E. A. (2000) A novel B lymphocyte-associated adaptor protein, Bam32, regulates antigen receptor signaling downstream of phosphatidylinositol 3-kinase. *J. Exp. Med.* **191**, 1319–1332
- Anderson, K. E., Lipp, P., Bootman, M., Ridley, S. H., Coadwell, J., Ronnstrand, L., Lennartsson, J., Holmes, A. B., Painter, G. F., Thuring, J. et al. (2000) DAPP1 undergoes a PI3-kinase-dependent cycle of plasma-membrane recruitment and endocytosis upon cell stimulation. *Curr. Biol.* **10**, 1403–1412
- Rodrigues, G. A., Falasca, M., Zhang, Z., Ong, S. H. and Schlessinger, J. (2000) A novel positive feedback loop mediated by the docking protein Gab1 and phosphatidylinositol 3-kinase in epidermal growth factor receptor signaling. *Mol. Cell Biol.* **20**, 1448–1459
- Venkateswarlu, K., Oatey, P. B., Tavare, J. M., Jackson, T. R. and Cullen, P. J. (1999) Identification of centaurin- α 1 as a potential *in vivo* phosphatidylinositol 3,4,5-trisphosphate-binding protein that is functionally homologous to the yeast ADP-ribosylation factor (ARF) GTPase-activating protein, Gcs1. *Biochem. J.* **340**, 359–363
- Gray, A., van der Kaay, J. and Downes, C. (1999) The pleckstrin homology domains of protein kinase B and GRP1 (general receptor for phosphoinositides-1) are sensitive and selective probes for the cellular detection of phosphatidylinositol 3,4-bisphosphate and/or phosphatidylinositol 3,4,5-trisphosphate *in vivo*. *Biochem. J.* **344**, 929–936
- Baraldi, E., Carugo, K. D., Hyvonen, M., Surdo, P. L., Riley, A. M., Potter, B. V., O'Brien, R., Ladbury, J. E. and Saraste, M. (1999) Structure of the PH domain from Bruton's tyrosine kinase in complex with inositol 1,3,4,5-tetrakisphosphate. *Structure Fold Des.* **7**, 449–460
- Ferguson, K. M., Kavran, J. M., Sankaran, V. G., Fournier, E., Isakoff, S. J., Skolnik, E. Y. and Lemmon, M. A. (2000) Structural basis for discrimination of 3-phosphoinositides by pleckstrin homology domains. *Mol. Cell* **6**, 373–384
- Lietzke, S. E., Bose, S., Cronin, T., Klarlund, J., Chawla, A., Czech, M. P. and Lambright, D. G. (2000) Structural basis of 3-phosphoinositide recognition by pleckstrin homology domains. *Mol. Cell* **6**, 385–394
- Ferguson, K. M., Lemmon, M. A., Schlessinger, J. and Sigler, P. B. (1994) Crystal structure at 2.2 Å resolution of the pleckstrin homology domain from human dynamin. *Cell (Cambridge, Mass.)* **79**, 199–209
- Dowler, S., Currie, R. A., Campbell, D. G., Deak, M., Kular, G., Downes, C. P. and Alessi, D. R. (2000) Identification of pleckstrin-homology-domain-containing proteins with novel phosphoinositide-binding specificities. *Biochem. J.* **351**, 19–31
- Otwinowski, Z. and Minor, W. (1997) Processing of X-ray diffraction data collected in oscillation mode. *Methods Enzymol.* **276**, 307–326
- Navaza, J. (1994) AMoRe: an automated package for molecular replacement. *Acta Crystallogr., Sect. A: Found. Crystallogr.* **50**, 157–163
- Perrakis, A., Morris, R. and Lamzin, V. S. (1999) Automated protein model building combined with iterative structure refinement. *Nat. Struct. Biol.* **6**, 458–463
- Jones, T. A., Zou, J. Y., Cowan, S. W. and Kjeldgaard, M. (1991) Improved methods for building protein models in electron density maps and the location of errors in these models. *Acta Crystallogr., Sect. A: Found. Crystallogr.* **47**, 110–119
- Sheldrick, G. M. and Schneider, T. R. (1997) SHELXL: High-resolution refinement. *Methods Enzymol.* **277**, 319–343
- Nicholls, A., Sharp, K. and Honig, B. (1991) Protein folding and association – insights from the interfacial and thermodynamic properties of hydrocarbons. *Proteins* **11**, 281–296
- Mao, Y., Nickitenko, A., Duan, X., Lloyd, T. E., Wu, M. N., Bellen, H. and Quioco, F. A. (2000) Crystal structure of the VHS and FYVE tandem domains of Hrs, a protein involved in membrane trafficking and signal transduction. *Cell (Cambridge, Mass.)* **100**, 447–456
- Holm, L. and Sander, C. (1993) Protein structure comparison by alignment of distance matrices. *J. Mol. Biol.* **233**, 123–138
- Laskowski, R. A., McArthur, M. W., Moss, D. S. and Thornton, J. M. (1993) Procheck: a program to check the stereochemical quality of protein structures. *J. Appl. Crystallogr.* **26**, 283–291
- Deak, M., Casamayor, A., Currie, R. A., Downes, C. P. and Alessi, D. R. (1999) Characterisation of a plant 3-phosphoinositide-dependent protein kinase-1 homologue which contains a pleckstrin homology domain. *FEBS Lett.* **451**, 220–226
- Salmeen, A., Andersen, J. N., Myers, M. P., Tonks, N. K. and Barford, D. (2000) Molecular basis for the dephosphorylation of the activation segment of the insulin receptor by protein tyrosine phosphatase 1b. *Mol. Cell* **6**, 1401–1412

Received 24 May 2001/20 June 2001; accepted 4 July 2001